

# Microfluidic Models of Vascular Functions

Keith H.K. Wong,<sup>1</sup> Juliana M. Chan,<sup>2,3</sup>  
Roger D. Kamm,<sup>3,4</sup> and Joe Tien<sup>1</sup>

<sup>1</sup>Department of Biomedical Engineering, Boston University, Boston, Massachusetts 02215; email: jtien@bu.edu

<sup>2</sup>Molecular Engineering Lab, Agency for Science Technology and Research, Singapore 138668

<sup>3</sup>Department of Biological Engineering and <sup>4</sup>Department of Mechanical Engineering, Massachusetts Institute of Technology, Cambridge, Massachusetts 02139; email: rdkamm@mit.edu

Annu. Rev. Biomed. Eng. 2012. 14:205–30

First published online as a Review in Advance on April 23, 2012

The *Annual Review of Biomedical Engineering* is online at [bioeng.annualreviews.org](http://bioeng.annualreviews.org)

This article's doi:  
10.1146/annurev-bioeng-071811-150052

Copyright © 2012 by Annual Reviews.  
All rights reserved

1523-9829/12/0815-0205\$20.00

## Keywords

vascular models, microcirculation, tissue engineering, chemical gradients, tumor angiogenesis, microfluidic hydrogels

## Abstract

In vitro studies of vascular physiology have traditionally relied on cultures of endothelial cells, smooth muscle cells, and pericytes grown on centimeter-scale plates, filters, and flow chambers. The introduction of microfluidic tools has revolutionized the study of vascular physiology by allowing researchers to create physiologically relevant culture models, at the same time greatly reducing the consumption of expensive reagents. By taking advantage of the small dimensions and laminar flow inherent in microfluidic systems, recent studies have created in vitro models that reproduce many features of the in vivo vascular microenvironment with fine spatial and temporal resolution. In this review, we highlight the advantages of microfluidics in four areas: the investigation of hemodynamics on a capillary length scale, the modulation of fluid streams over vascular cells, angiogenesis induced by the exposure of vascular cells to well-defined gradients in growth factors or pressure, and the growth of microvascular networks in biomaterials. Such unique capabilities at the microscale are rapidly advancing the understanding of microcirculatory dynamics, shear responses, and angiogenesis in health and disease as well as the ability to create in vivo–like blood vessels in vitro.

## Contents

INTRODUCTION.....	206
ADVANTAGES OF MICROFLUIDIC CELL CULTURE.....	207
SCOPE OF THE REVIEW.....	207
MICROFLUIDIC STUDIES OF HEMODYNAMICS.....	207
Hemodynamics in Normal Physiology.....	209
Hemodynamics in Pathophysiology.....	210
MICROFLUIDIC APPLICATION OF SHEAR.....	210
Throughput Enhancement.....	211
Endothelial Barrier Function.....	212
Red Blood Cells Under Shear.....	213
Blood Coagulation.....	214
ANGIOGENESIS AND CO-CULTURE UNDER DEFINED MICROENVIRONMENTS.....	214
Angiogenesis Under Defined Gradients and Flow.....	215
Angiogenesis in Co-Culture.....	217
Other Co-Culture Models.....	217
VASCULAR FUNCTION AND TRANSPORT IN MICROFLUIDIC HYDROGELS.....	218
Microfluidic Scaffolds for Tissue Engineering.....	218
Functional Vascularization of Microfluidic Scaffolds.....	220
FUTURE DIRECTIONS.....	222
Filling in the Missing Pieces for a “Complete” Microvessel.....	223
Toward Functional Microvascular Beds and Tissue-Engineered Organs.....	223

## INTRODUCTION

Since the isolation of endothelial cells (ECs), smooth muscle cells (SMCs), and pericytes in the 1970s and 1980s (1–4), vascular physiology has been studied *in vitro*, usually with cultures on plates, filters, or hydrogels. These centimeter-scale cultures have greatly advanced our understanding of how the vascular system functions in healthy and diseased states. Areas of particular interest include the regulation of angiogenesis (5), the response of vascular tone to shear stress (6), the adhesion and transmigration of leukocytes during inflammation (7), the prevention of thrombus formation (8), the regulation of vascular permeability (9), and ischemia/reperfusion injury (10).

In exchange for experimental convenience, many of these *in vitro* models sacrifice physiological accuracy. For instance, they often place vascular cells on two-dimensional (2D) plastic substrates that are much stiffer than native tissues, or in three-dimensional (3D) hydrogels that display nonphysiological porosities and compositions. Interstitial flow (11) and growth factor gradients (12), factors that regulate microvascular growth *in vivo*, are typically absent. Most studies do not provide a constant flow over vascular cells; even fewer provide pulsatile stress to mimic the pressure or flow waveforms experienced by cells *in vivo*. Moreover, *in vitro* culture raises the basal turnover rate of ECs from ~0.1% per day *in vivo* to 1–10% per day (13). Nonphysiological features of the cell culture environment, such as supraphysiological oxygen levels and high growth factor concentrations in serum, are present even in the most sophisticated *in vitro* culture systems.

**EC:** endothelial cell

**SMC:** smooth muscle cell

## ADVANTAGES OF MICROFLUIDIC CELL CULTURE

In this review, we highlight recent advances in the application of microfluidic systems to studies of vascular function. Most of these studies used photolithography or soft lithography to fabricate patterned microfluidic channels with micrometer resolution [e.g., in the elastomer polydimethylsiloxane (PDMS)]. Because the smallest dimensions in microfluidic devices are less than 1 mm, the Reynolds numbers ( $Re$ ) of the flows are typically small ( $<10$ , and often much less) and the flows are inherently laminar. Fluid physics and transport phenomena in such low  $Re$  flow are very well characterized (14, 15). Coupled with innovative techniques for handling fluids, laminar flow allows the precise patterning of fluid streams (16, 17). Microfluidic systems are thus particularly well suited for exposing cultured vascular cells to actively modulated, locally heterogeneous, and precisely controlled flow environments. At the same time, microfluidic cultures facilitate high-throughput experimentation by greatly reducing the consumption of expensive reagents and cells and by allowing the integration of detection assays directly in the microfluidic material (e.g., transparent PDMS). Moreover, the high resolution of lithography enables the formation of microfluidic systems that mimic the geometry of microvascular beds.

In some microfluidic systems, cells that are plated in the micropatterned channels are grown adjacent to regions that contain 3D matrices or adjacent to other regions that contain different cell types (18). The sprouting of microvessels into the matrix under different chemical or physical local microenvironments can be closely regulated to mimic *in vivo* conditions. Close investigation of the growth of these vascular structures is also possible via high-resolution, time-lapse imaging.

---

**PDMS:**  
polydimethylsiloxane  
**RBC:** red blood cell

---

## SCOPE OF THE REVIEW

Rather than exhaustively document microfluidics-based studies of vascular physiology, we have organized this review around the microfluidic configuration used and the associated advantage for study of the vascular system. This review covers work in four areas of recent interest: (a) blood circulation at the microvascular scale, (b) behavior of the endothelium and blood cells under applied shear stress, (c) angiogenesis and co-culture assays in defined microenvironments, and (d) vascularization of microfluidic scaffolds (**Figure 1**). Implicit in this organization is the recognition that no single microfluidic system is likely to be useful for modeling all vascular functions. We conclude with a discussion of the current limitations of microfluidics-based studies and how one might overcome them.

## MICROFLUIDIC STUDIES OF HEMODYNAMICS

Blood circulation has long been a topic of interest in biomechanics with an extensive history of experimental and theoretical investigations. Early experimental studies of the microcirculation were performed in kinematically and dynamically similar systems on the centimeter scale (19, 20) or in glass capillary tubes (21). Dynamically similar systems, scaled using principles of continuum mechanics based on the Reynolds number ( $Re = VD/\nu$ , where  $V$  is a characteristic flow velocity,  $D$  the vessel diameter, and  $\nu$  the kinematic viscosity of blood) and Womersley number [ $\alpha = (D/2)\sqrt{\omega/\nu}$ ], where  $\omega$  is a characteristic frequency of flow unsteadiness], are useful when studying relatively simple situations such as the shear force acting on a single cell (20) or more complex problems such as unsteady flow in nonuniform geometries (22).

The validity of these scaling approaches as well as that of the continuum assumption, however, breaks down when discrete red blood cells (RBCs), cell-cell interactions, or molecular signaling gains significance in microcirculatory dynamics. For instance, flowing RBCs tend to aggregate in

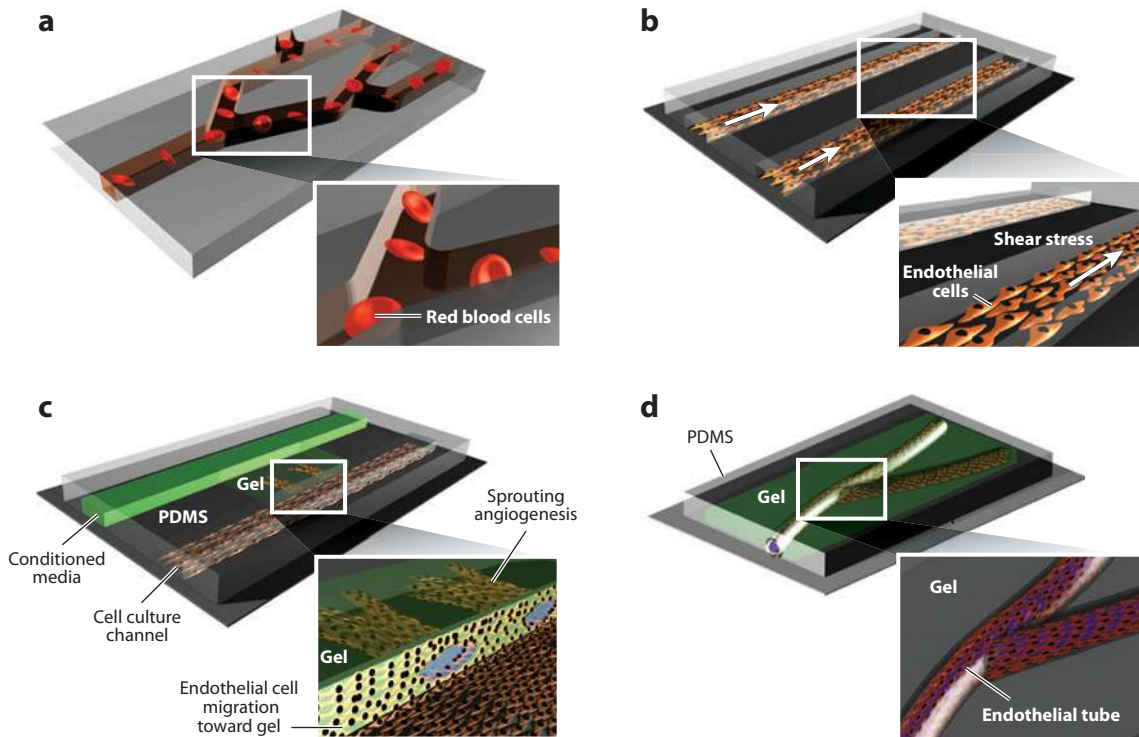


**Figure 1**

Microfluidic models of vascular functions. (a) Construction of flow networks to study hemodynamics in microcirculation.

(b) Application of shear stress to study vascular cell biology. (c) Microfluidic patterning of cells and fluid streams to create defined microenvironments, such as a chemical gradient. (d) Vascularization of microfluidic channels to form microvascular networks within hydrogels. Abbreviation: PDMS, polydimethylsiloxane.

the center of microvessels (vessels that are less than  $\sim 100 \mu\text{m}$  in diameter), leaving a cell-free zone near the vessel wall and decreasing the apparent viscosity (the Fåhræus-Lindqvist effect) (23). Cell-cell adhesion and RBC flexibility together give rise to the non-Newtonian behavior of blood in which the apparent viscosity decreases with increasing shear rate, reaching a constant value of 3–4 cP above a shear rate of  $\sim 100 \text{ s}^{-1}$ . Furthermore, as the size scale further decreases to single-RBC flow in capillaries, cell–vessel wall interactions should also be considered. At this scale, the glycocalyx, a glycoprotein and glycolipid layer that coats ECs *in vivo*, takes on increased importance and influences a variety of phenomena including the radial distribution of RBCs, pressure–flow relationships, and transendothelial exchange [see Weinbaum et al. (24) for a comprehensive review]. On the one hand, given all these complicating factors, it is difficult to see how dynamic scaling can be applied generally to reproduce microvascular hemodynamics using centimeter-scale experiments. On the other hand, it is technically challenging to form flow networks representative of *in vivo* microvascular beds using single glass capillary tubes, which also present the cells a much stiffer substratum compared with subendothelial basement membrane and tissue *in vivo*.

Because flow networks on the 5–100- $\mu\text{m}$  scale of the microvasculature are reproducibly fabricated by photolithography, lithographically formed microfluidic systems have opened the door to studies on microcirculatory dynamics. Here, microfluidic systems are functionally “passive”: They are simply meant to replicate the geometry of the microcirculation. Construction of

microfluidic channels for early studies of blood flow was accomplished by etching glass or silicon substrates (25). The lengthy fabrication processes likely limited widespread use of these methods until PDMS-based rapid prototyping gained popularity (26).

## Hemodynamics in Normal Physiology

The first PDMS-based model of the microcirculation (27) reproduced RBC deformation observed *in vivo*; this morphological change is believed to facilitate gas exchange *in vivo* by increasing the surface area of the RBC in contact with the capillary endothelium and by generating steep transport gradients within the thin region between the RBC and the wall. RBCs, normally 7–8  $\mu\text{m}$  in diameter, deformed into a parachute-like shape in slightly wider channels or into a bullet shape in slightly narrower ones (**Figure 2a**). When RBCs are forced through very narrow channels ( $\leq 3 \mu\text{m}$ ), their membrane mechanics takes on greater significance and the relationship between pressure drop and RBC flow velocity becomes highly sensitive to changes in temperature (28). This study (28) pointed out another important function of microfluidic experiments: validating

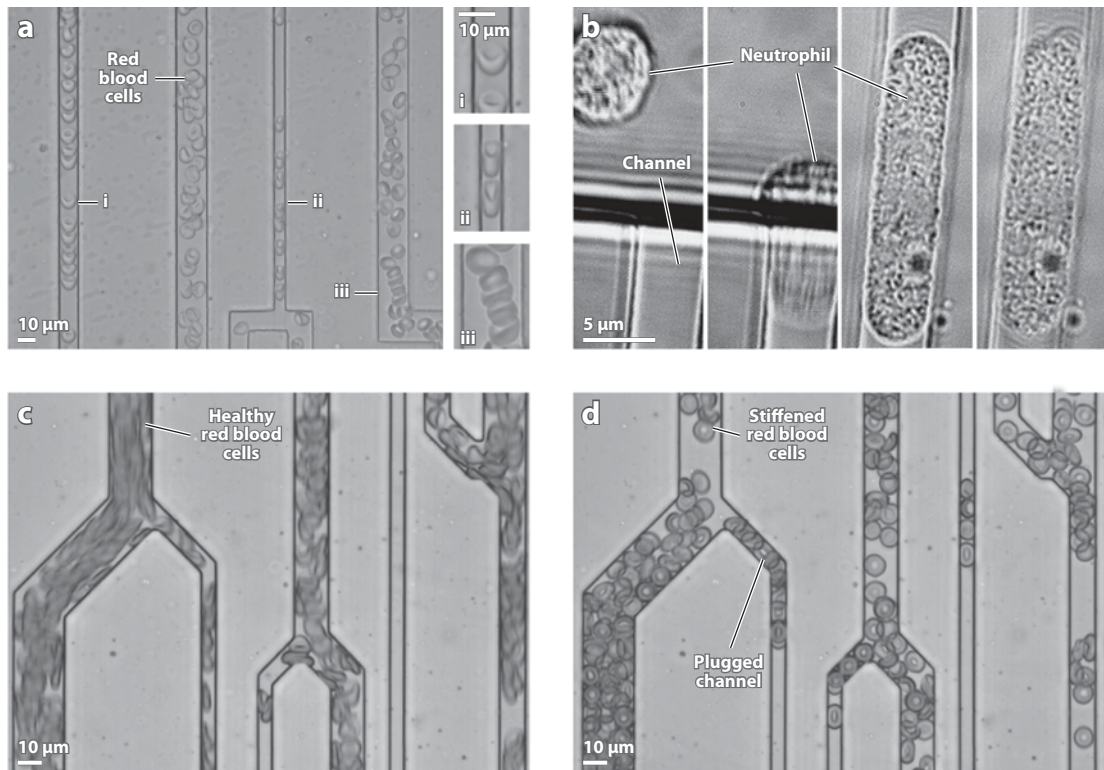


**Figure 2**

Microfluidic studies of microcirculatory dynamics. (a) Red blood cells (RBCs) deformed into a parachute shape (i) or bullet shape (ii), or they formed rouleaux (iii) in channels of different widths. Modified with permission from Elsevier (27). (b) A neutrophil that was forced into a capillary channel. Granule tracking revealed rheological changes under deformation. Modified with permission from the American Physiological Society (29). Perfusion of healthy (c) and stiffened (d) RBCs. RBC stiffening caused plugging of microchannels. Modified with permission from the Royal Society of Chemistry (45).

**Leukostasis:**  
pathological  
aggregation of  
leukocytes in the  
bloodstream, usually  
in the context of  
leukemia

computational models of single-cell mechanics. Other hemodynamic phenomena, such as plasma skimming and flow reversal, were also observed in these flow networks (27).

Microfluidic channels have also been used to study the deformation of leukocytes such as neutrophils. For instance, when forced into channels on the scale of small capillaries, neutrophils transiently decrease their mechanical stiffness (**Figure 2b**) (29). This change in stiffness was due in part to actin depolymerization on short (approximately seconds) timescales (30); within minutes, the cell stiffness recovered to predeformation levels.

The stiffer and larger leukocytes, when interacting with RBCs, give rise to interesting microvascular flow phenomena. For example, because RBCs are typically much more abundant than leukocytes, the fast-flowing RBCs in the core of the vessel collide with leukocytes and force them toward the vessel wall in a process known as margination. This process, which promotes leukocyte-EC contact and adhesion (22), was studied in bifurcating channels (31) and sudden expansions (32); the latter geometry could model local enlargement of the lumen in dilated postcapillary venules during inflammation. A similar phenomenon occurs in capillary sprouts, where leukocytes are pushed into dead-end, no-flow bifurcations (33).

## Hemodynamics in Pathophysiology

Microfluidic systems are also used to model blood cell pathology. Clinically, alterations in blood cell deformability and complications in microvascular perfusion occur in diseases such as leukostasis in leukemia (34), sickle cell disease (35), sepsis (36), malaria (37), and diabetes (38). Blood cell rheology has traditionally been studied using cone-and-plate viscometry (39) or filtration through micropores (40). Of note, cone-and-plate viscometry showed a significant effect of diamide, a common RBC stiffening agent, on the reduction in RBC deformation (39, 41), whereas *in vivo* studies suggested that such effects on the pressure-flow relationship in capillary networks are minimal (42, 43). Microfluidic experiments (44) have produced results consistent with *in vivo* studies, and the authors attributed this finding to the more physiological pressure-driven flow in channels versus the flow in cone-and-plate shearing.

An important rationale for using microfluidic systems lies in the ability of researchers to visualize directly the effects of stiffened cells on perfusion in the entire flow network (45), a dynamic observation that is not possible in filtration or viscometer studies (**Figure 2c,d**). In a model of sickle cell crisis that integrated molecular, cellular, and tissue-level dynamics, sickled RBCs were deoxygenated across a gas-permeable PDMS membrane, causing polymerization of hemoglobin S, followed by cell stiffening and subsequent flow occlusion. Rescue after reoxygenation was possible, and therapeutic red cell exchange delayed occlusion (46). Likewise, the stiffening of neutrophils by the inflammatory mediator N-formyl-methionyl-leucylphenylalanine increased their transit time in channels having a width of 6  $\mu\text{m}$  and height of 13  $\mu\text{m}$ . When cells taken from leukemia patients showing symptoms of leukostasis were added to the devices, flow in the channels was impaired owing to the presence of a subpopulation of cells with relatively long transit times (47); these results have clinical implications in acute leukemia when leukocyte concentration increases quickly (48).

## MICROFLUIDIC APPLICATION OF SHEAR

In the mammalian vascular system, blood-flow patterns and the resulting fluid shear on vascular walls are extremely heterogeneous, ranging from pulsatile flow in large and small arteries to slow or intermittent flow in capillaries and veins. Average shear stresses are higher in the arterioles and capillaries, on the order of 40–60  $\text{dyn cm}^{-2}$ , and lower in large arteries and venules, on the order

of 10–20 dyn cm<sup>-2</sup> (49). However, transient shear stress on the order of 200 dyn cm<sup>-2</sup> may occur in large arteries for short periods during systole. Significant spatial variations also exist, especially in cases of arterial occlusion.

Studies of the vascular response to shear stress have broad clinical relevance in vascular homeostasis and pathophysiology. For instance, the disturbed flow that is often present near bifurcating vessels causes low or unsteady shear levels that induce ECs to adopt an atherogenic phenotype (50). Therefore, *in vitro* models of endothelium often attempt to create steady, pulsatile, or disturbed (e.g., complex secondary, reversing, or turbulent) flow patterns. Traditionally, shear stress can be applied to the vascular endothelium using parallel-plate flow chambers or viscometers, which can generate shear stress uniformly or with spatial gradients within the same endothelial monolayer. With the introduction of microfluidic devices that apply shear to cells, substantial improvements in experimental versatility and throughput are now possible.

### Throughput Enhancement

For the application of shear stress, microfluidic systems do not necessarily possess closer physiological relevance over macroscale systems. In fact, macroscale systems (e.g., cone-and-plate viscometers and parallel-plate devices) have been very successful in dissecting the changes in ECs under shear, leading to great advances in our understanding of the progression and anatomical localization of vascular diseases (50, 51). Viewed in this light, a major advantage of microfluidics in shear experiments is enhanced throughput. To put numbers into context, it is useful to consider the relationship between shear stress and volumetric flow rate: For Poiseuille flow in circular channels, the shear stress scales as  $\tau \sim Q/r^3$ , where  $Q$  is the volumetric flow rate and  $r$  is the vessel radius; for channels of rectangular cross section with height  $b$  and width  $w$ ,  $\tau \sim Q/w \cdot b^2$ . In other words, by shrinking the device by 100-fold—for example, from centimeter-scale flow chambers to 100- $\mu$ m-scale microchannels—one can achieve the same level of shear stress with a flow rate that is nearly 1 million times smaller.

This great reduction in flow rate per channel has made it possible to perform assays in a high-throughput manner. For instance, shear stress levels ranging from 0.7 to 130 dyn cm<sup>-2</sup> were applied simultaneously in a single chip containing ten microscale flow chambers, each 200- $\mu$ m wide and 100- $\mu$ m tall (52). In another study, a microscale parallel-plate flow chamber generated a linear gradient of shear along the same monolayer (53). This configuration took advantage of the very thin flow chamber height (100  $\mu$ m) compared with the lateral dimensions to justify the use of Hele-Shaw flow theory to calculate the flow field. This study showed that tumor necrosis factor alpha (TNF- $\alpha$ )-induced VCAM-1 and E-selectin expression were upregulated at low shear levels (2–4 dyn cm<sup>-2</sup>) and suppressed at high shear levels (>8 dyn cm<sup>-2</sup>). It also showed that monocytes preferentially adhered to low-shear regions; the configuration of the microfluidic device allowed well-controlled comparisons across multiple levels of shear in a single experiment.

One novel demonstration of the versatility of microfluidic technology is the refreshable Braille display-controlled chip developed by Takayama and coworkers. In this device, piezoelectric pins from a Braille display are programmed to actuate valves and peristaltic pumps in PDMS microfluidic devices by pushing against an elastic PDMS membrane (54). Appropriate valving and reverse-pumping cycles allowed mixing of microfluidic streams even under low Reynolds numbers. In these studies, the microfluidic device is no longer passive and instead actively drives flow through external actuation. In theory, the throughput of this automated assay is limited only by the number of pins, although the discrete nature of the activation inevitably gives rise to some degree of flow pulsatility. Using different pump sizes and frequencies of actuation provided a means to study the effect of pulsatile shear on EC shape and alignment (**Figure 3a**) (55).

---

**Hele-Shaw theory:**  
an approximation of fluid flow in a narrow gap between parallel plates by 2D potential flow

---

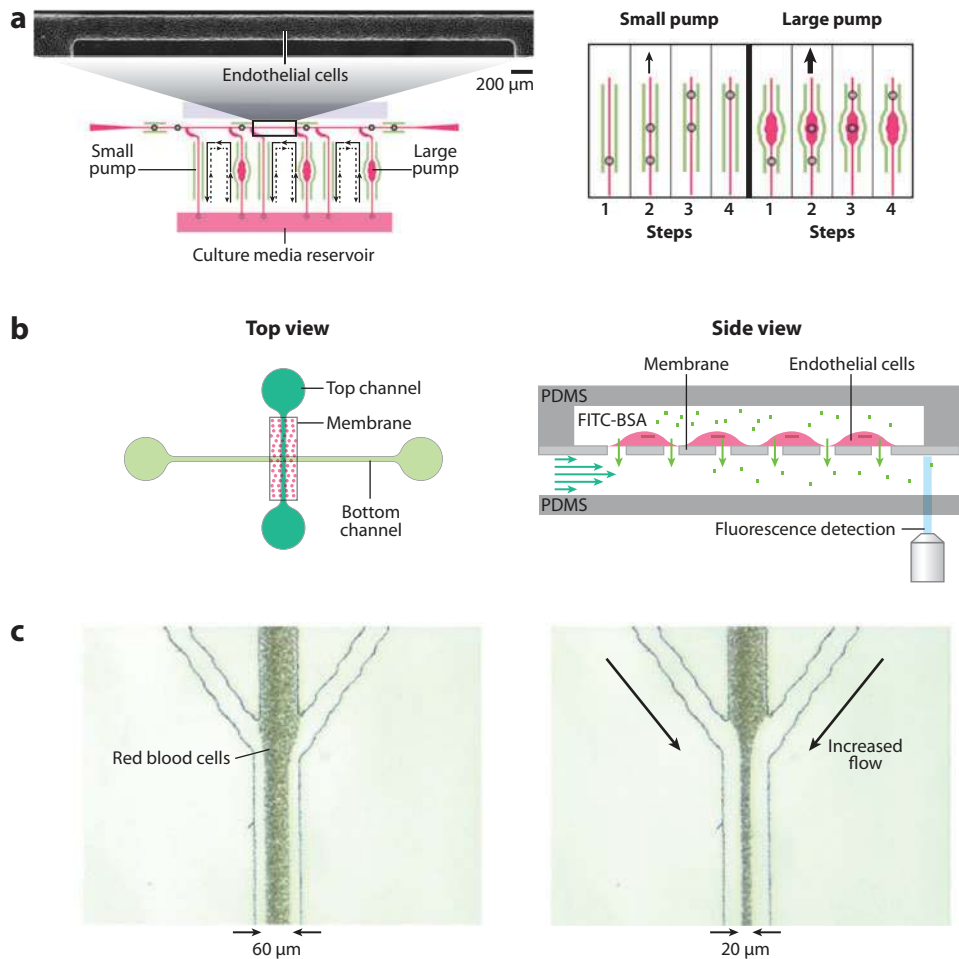


**Figure 3**

Microfluidic shearing. (a) Endothelial cell (EC)-culture chamber sheared by Braille pin-actuated microfluidic pumps (*left*). Illustration of the three-pin, peristaltic pumping sequence of the small and large pumps that results in pulsatile flow (*right*). Modified with permission from the American Chemical Society (55). (b) The study of barrier function using ECs cultured on a membrane that is sandwiched between two microfluidic flow chambers. Extravasated albumin is detected with fluorescence microscopy. Modified with permission from the American Chemical Society (59). (c) Hydrodynamic focusing from three converging streams caused shearing of red blood cells in the central stream. Modified with permission from the Royal Society of Chemistry (68). Abbreviations: FITC-BSA, fluorescein isothiocyanate-labeled bovine serum albumin; PDMS, polydimethylsiloxane.

## Endothelial Barrier Function

In the context of vascular physiology, barrier function refers to the ability of the vessel wall to restrict passage of macromolecules, ions, and water, chiefly across the endothelium and its glycocalyx (9). Regulation of endothelial permeability is important for maintaining water and solute balance during normal homeostasis, while allowing rapid exchange during inflammation (56). Early studies of permeability *in vitro* relied on measurements of water or solute flux across a confluent endothelium on porous filters that served both as cell-culture substrates and as membranes that



permitted transport of the molecule of interest (57). Subsequent addition of a flow chamber atop the filter system to impart physiological flow to the endothelium revealed the shear dependence of permeability (58).

Microfluidic implementation of the permeability assay made use of similar arrangements by sandwiching porous filters between PDMS-based microfluidic channels with controlled flow rates (**Figure 3b**) (59). Another version eliminated the filters; instead, a short (2- $\mu\text{m}$  high) gap in the PDMS device served as a barrier to endothelial migration, while allowing extravasation of albumin and calculation of permeability coefficients by fluorescence microscopy (60); this setup provides a particularly simple device to measure permeability under pulsatile and oscillatory shear stress. Other microfluidic studies of barrier function include the use of a neighboring fluidic compartment for histamine stimulation (61) and a miniaturization of circuitry for the measurement of transendothelial electrical resistance (62). Although these studies did not focus on shearing the endothelium, addition of such capabilities should be straightforward.

---

**ATP:** adenosine triphosphate

**NO:** nitric oxide

---

### Red Blood Cells Under Shear

Apart from the endothelium, other components in the blood stream are also subject to fluid shear. Adenosine triphosphate (ATP), believed to act as a vasodilator (63), is released from RBCs when they are forced through filters (64) or under flow in microbore tubings with diameters ranging from 25  $\mu\text{m}$  to 75  $\mu\text{m}$  (65). Microfluidic channels have been applied to study this release in a variety of configurations (66). Devices that contained narrowing channels were used to show higher ATP release in narrower segments of the same flow channel (67). Subsequent studies used hydrodynamic focusing to change the fluid shear rate; here, increasing the flow rate of adjacent streams caused RBCs to flow in a narrower stream, thus generating higher local shear rates and resulting in greater ATP release (**Figure 3c**) (68). This work demonstrates the unique advantage in lithography-based microfluidics over glass capillary tubes in the routine construction of interconnected flow channels.

An important advantage of PDMS-based microfluidics in this area is their transparency, which enables ready optical imaging of dynamic phenomena at different positions in the device. Correlation of the observed cell behavior with the local shear environment can then allow the study of cell behavior during rapid changes in shear. Recent studies used this strategy to uncover the existence of a time delay from the onset of RBC shearing to ATP release (69, 70). Surprisingly, ATP release is prevented if RBCs are allowed to recover quickly to their original shape (70). High-throughput time-lapse imaging in such microfluidic devices, coupled with traditional cone-and-plate viscometry, shed light on the link between RBC deformation, bulk viscosity, and ATP release (69). Researchers determined that flow was required for a basal level of ATP release, but shear stress dependence of ATP release was not observed until shear exceeded  $\sim 30 \text{ dyn cm}^{-2}$ . Fast imaging of RBC dynamics under flow channels revealed that shear thinning of blood—a non-Newtonian fluid behavior in which increased shear causes a decrease in apparent viscosity—was not due to RBC deformation, in contrast to common belief (71). Rather, shear thinning appeared to result from a shear-induced reduction in the fraction of RBCs that underwent rigid body rotation.

The transparency of PDMS-based microfluidics also enables on-chip chemiluminescence assays. The ATP that is released from sheared RBCs causes local release of nitric oxide (NO) from nearby ECs (64). Given that endothelial-derived NO is responsible for smooth muscle relaxation (72), *in vitro* co-cultures of RBCs, ECs, and SMCs under flow represent an attractive model for further exploration of vasomotion dynamics. Although such a complex tissue model has yet to be realized, many of the analytical techniques for biochemical analysis of ATP and NO levels in the microfluidic setting have been developed. Because NO's half-life is short (on the order of minutes) (73), direct measurements in a continuous flow system are advantageous (74). Measurements of

**Tissue factor:**

a membrane protein that serves to catalyze the formation of fibrin clots in the extrinsic pathway of coagulation

**ECM:** extracellular matrix

**VEGF:** vascular endothelial growth factor

**S1P:** sphingosine 1-phosphate

endothelium-derived NO on-chip in microfluidic systems have been obtained with carbon microelectrodes (75) or fluorescence microscopy (76). Using the latter method, Spence and coworkers cultured ECs on porous membranes and perfused RBCs through underlying microfluidic channels; they showed that ATP that is released from iloprost-stimulated RBCs upregulated NO production in ECs (77). In a similar system, estradiol inhibited ATP release from RBCs, in turn decreasing endothelial NO production (78). By measuring transendothelial electrical resistance, researchers have been able to assess endothelial barrier function in the presence of flowing RBCs (79).

## Blood Coagulation

Thrombosis dynamics are also affected by flow (80). Microfluidic devices have been designed to study the propagation of an upstream preformed clot to a downstream abrupt expansion that simulated a venous valve; recirculating flow in the valve increased the residence time of blood plasma and allowed real-time observation of clot propagation (81). The clot, positioned at a fluidic branch perpendicular to the major flow channel, was first initiated using predeposited tissue factor. Under low flow, this clot front advanced into the flow channel and was carried downstream, initiating another clot at the valve within 10 min. Shear rates greater than  $90 \text{ s}^{-1}$  delayed clotting in the valve to  $>30$  min. This work is consistent with the theory that clotting requires clot-initiating agents to exceed a certain threshold concentration (82), because high shear rate effectively dilutes their local concentration.

A subsequent study used capillary tubes precoated with a small patch of tissue factor to initiate the clot (83). Systematic variation of diameter and flow rates showed that the wall shear rate, rather than volumetric flow or flow velocity, governed the clotting dynamics. Delay of clotting under high shear rate was reproduced in platelet-rich plasma as well as whole blood, although a threshold was difficult to quantify in the latter owing to its fast spontaneous clot times ( $\sim 10$  min) (83).

## ANGIOGENESIS AND CO-CULTURE UNDER DEFINED MICROENVIRONMENTS

Cells *in vivo* reside in a complex 3D architecture, respond to cues from the extracellular matrix (ECM), undergo cell-cell chemo-mechanical coupling, and respond to morphogen concentrations and gradients. Spatiotemporal resolution of growth factors, either uniformly distributed or in gradients, is important for microvascular function *in vivo*. Vascular endothelial growth factor (VEGF) is a fundamental regulator of vascular angiogenesis and lymphangiogenesis in vertebrates, in concert with a multitude of other growth factors, such as platelet-derived growth factor B, transforming growth factor beta 1, fibroblast growth factor 2 (FGF2), sphingosine 1-phosphate (S1P), and angiopoietins (Ang1, Ang2), as well as signaling pathways involving Notch and ephrins in ECs (84). Whereas VEGF acts as a critical morphogen, other factors such as FGF2 act primarily as a mitogen (85). Gradients in VEGF are routinely established *in vivo* through the presentation of distinct VEGF isoforms with different affinities for heparin-rich matrix components or owing to spatial variations in synthesis and secretion rates (12). These VEGF gradients are necessary for proper vessel patterning in the retina as demonstrated in VEGF<sup>F120/120</sup> mice, which lack heparin-binding VEGF isoforms (86).

Growth factor expression and activity also show temporal profiles. At the earliest stage, VEGF and S1P stimulate endothelial morphogenesis, making them the prime effectors of the neovascularization that occurs in embryonic development and in association with various pathologies (87). In murine xenograft and allograft models, administration of an anti-S1P monoclonal antibody

arrested the ability of VEGF and bFGF to induce tumor-associated angiogenesis (88). Targeted gene-inactivation studies in mice have shown that VEGF is necessary for the early stages of vascular development, whereas the angiopoietins such as Ang1 are required for the later stages of vascular remodeling (89). In mRNA profiling studies, Ang1 mRNAs were upregulated in cultured serum-starved retinal pigment epithelium cells by VEGF in a time- and dose-dependent manner (90).

Angiogenesis has been studied *in vitro* since ECs were first observed to form networks and tube-like structures (91). In the earliest studies by Folkman & Haudenschild (91) in 1980, tumor cells were cultured separately to generate conditioned tumor medium for EC cultures. Later versions for *in vitro* co-culture and gradient generation include trans-filter assays in Boyden chambers to juxtapose ECs on one side with tumor or mesenchymal cells on the other (92). These assays in studying paracrine interactions, however, give discrete, quantitative end-point data of the transmigration of radiolabeled cells (e.g.,  $^{51}\text{Cr}$ ) in various growth factor gradients. Although it is possible to obtain a full data set using one sample per time point, these trans-filter assays do not allow for real-time imaging of the temporal profile within an individual sample.

To achieve conditions that are closer to physiological environments, researchers have used organ culture assays such as rat aortic ring explants and chick embryo aortic arch explants placed on Matrigel for 1–2 weeks to study the effects of angiogenic promoters and inhibitors in a 3D environment. These *in vitro* assays are described in detail in general reviews (5, 93, 94). Since then, researchers (95) have further studied angiogenesis by developing a number of advanced microfabrication techniques that enable independent variation of cell-cell, cell-ECM, and cell-soluble factor interactions.

## Angiogenesis Under Defined Gradients and Flow

Microfluidic devices are useful for studying the effect of chemical gradients within biological cultures *in vitro*. By controlling laminar flow streams in microfluidic chips with pumps and valves, investigators can circulate culture medium continuously for hours to weeks within these channels. Using these devices, researchers can generate a theoretically unlimited number of parallel streams. Owing to diffusion at the boundaries of narrow parallel layers, the formation of gradients is possible, which can be designed to be linear, parabolic, or periodic (96). The resulting stable gradients can be used to study the migration, proliferation, and differentiation of cells *in vitro*, such as the initiation of angiogenesis by ECs.

Other microfluidic chip designs have incorporated a hydrogel (e.g., collagen type I, fibrin, Matrigel) between two channels to observe the effect of chemical gradients across a gel that mimics the ECM *in vivo*. For example, in a microfluidic device with two channels flanking a gel region, an SIP concentration gradient was established across the collagen gel using dynamic flow conditions and was used to test how growth factor gradients perturb EC sprouting and migration (18). Other studies have similarly tested EC migration and capillary morphogenesis under stable VEGF gradients (**Figure 4a,b**) (97). In these studies, two types of endothelial invasion occurred: one with EC migration along the surfaces of the device, which later formed vascular lumens, and another in which the vascular structures emerged directly as sprouts into the gel matrix. Later studies demonstrated that the second, more natural form of angiogenesis could be promoted either by using stiffer matrices or by coating the PDMS surface with poly-D-lysine hydrobromide (98). These techniques have also been extrapolated to study the effect of gradients on whole tissues and organs. In one study, embryonic mouse kidneys and embryoid bodies were isolated and attached to a collagen I gel region flanked by microfluidic channels; VEGF and FGF gradients were set up across the tissues, and the gradients induced directional angiogenesis (99).

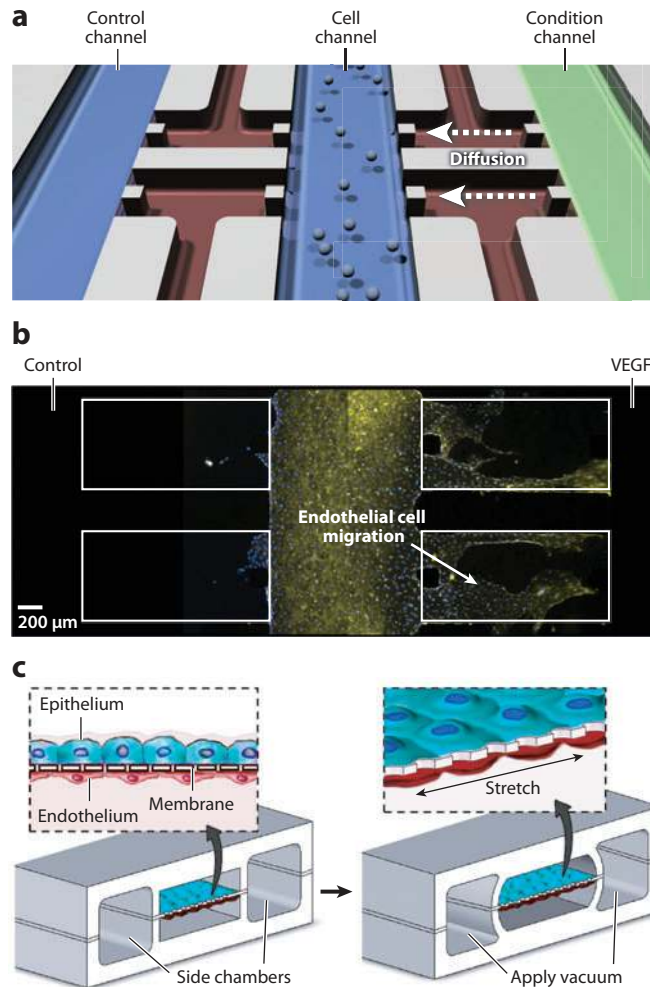


**Figure 4**

Control of microenvironments. (a) Microfluidic devices can be used to study paracrine interactions of endothelial cells (ECs) with vascular endothelial growth factor (VEGF) gradients in the media. (b) Microvascular ECs are cultured in the center channel, and VEGF is added to the right channel to create a gradient across the center and right channels. Modified with permission from the Royal Society of Chemistry (97). (c) Microfluidic reconstruction of the alveolar-capillary barrier. Application of vacuum on the side chambers mimicked breathing-induced stretch of the cell-culture membrane. Modified with permission from the American Association for the Advancement of Science (108).

Studies in postnatal mouse retina have shown that cells such as astrocytes provide spatial guidance for the patterning of microvascular networks into predetermined tracks (100). Hence, besides growth factor gradients, the contribution of spatially regulated EC binding sites can be studied using photopolymerizable polyethylene glycol polymers conjugated to adhesive RGD (Arg-Gly-Asp) ligands. When introduced from one of two inlets, the adhesive ligands deposit in a gradient that results from sequential merging, mixing, and splitting of the two streams. Once photo-crosslinked, the resultant hydrogels support a gradient of EC attachment that reflects the gradient of patterned adhesive ligands (101).

Intraluminal shear stress also influences angiogenesis, although two published studies report conflicting findings: In a macroscale system, one showed that shear enhances EC invasion in the presence of S1P (102); in a microfluidic system, the other showed inhibition of endothelial invasion by a NO-mediated mechanism (103). Microfluidics has also been used to investigate the effects of flow generated by pressure gradients across an endothelial monolayer, with and without differences in VEGF concentration across the gel region to which the monolayer is adhered (103). Effects of this transendothelial flow depend on flow direction, with basal-to-apical flows tending to enhance the invasion of ECs with extensive filopodial structures growing into the gel region. Such studies would not have been possible in conventional culture systems. The mechanisms responsible for these intriguing results, however, remain to be elucidated.

## Angiogenesis in Co-Culture

Traditional co-culture models either grow monolayers of cells on top of one another using transwell filter assays or use microprinting techniques, both of which give 2D environments. For 3D techniques, earlier studies of interactions with mural cells and ECs in spheroidal co-cultures showed how SMCs promote quiescent EC states, but these studies lacked precise spatial patterning and separation of cell types (104).

Microfluidic systems are capable of mimicking 3D tissue architecture by patterning cell-embedded gels with fine spatial and temporal control. One study examined the interaction between ECs placed on one side of a gel matrix while a SMC precursor cell line (10T1/2) was placed in the opposite channel, separated by approximately 1 mm. The 10T1/2 cells both helped to stabilize the monolayer and, in rare cases, attached to it (97). In another study, rat primary hepatocytes were cultured in one channel on the side of a collagen gel, with either rat or human microvascular ECs cultured across the gel in a second channel, allowing for direct communication between the two cell types (105). The hepatocyte cultures were influenced by morphogenetic cues from the ECs and vice versa, leading to extensive vascular sprouting from the EC monolayer, in the absence of any direct contact or mechanical interaction between the two cell types. Similar approaches were used to create a “perivascular niche,” composed of ECs suspended in fibrin gels adjacent to stromal cells such as fibroblasts or mesenchymal stem cells; here, the stromal cells promoted capillary morphogenesis in a manner that required stromal cell adhesion to EC-deposited laminin (106).

Other microfluidic configurations permit microscale co-cultures that have extensive heterotypic cell-cell contact. In one study, primary rat hepatocytes and ECs were allowed to form spheroids that were then deposited in an array of 0.3-mm-wide microreactors; a microporous filter held the cells in place. These co-cultures could be maintained by perfusion for up to two weeks, during which time the ECs organized into networks around the hepatocytes (107).

## Other Co-Culture Models

Other features of the *in vivo* microenvironment, such as cellular extravasation from circulation and physiological tissue movements (e.g., stretching), can also be modeled in microfluidic systems. Recently, a lung-on-a-chip model was proposed as an *in vitro* functional tissue mimic for applications such as drug screening (108). Here, researchers reconstituted the alveolar-capillary barrier of the lung by growing epithelial cells in air and ECs in culture media and by separating the two monolayers with a porous PDMS membrane. This air-liquid interface culture promoted alveolar-capillary barrier function, as measured by trans-bilayer electrical resistance and albumin transport. Application of a vacuum at the side chambers induced cyclic stretching of the porous

membrane that emulated physiological breathing deformations (**Figure 4c**). Another study that focused on spatial localization is the cancer metastasis model, in which two channels sandwiched a polyester porous membrane (109). The top layer contained a confluent EC monolayer, and the local chemokine stimulation of the endothelium from the bottom channel caused circulating cancer cells to adhere preferentially to these sites.

## VASCULAR FUNCTION AND TRANSPORT IN MICROFLUIDIC HYDROGELS

Recent studies have begun to build microfluidic networks into biomaterials that support 3D cell culture and vascular in-growth. These studies are motivated by the problem of vascularization when engineering large tissues. Because current methods for generating vascular networks rely on the sprouting of native vessels or on the tubulogenesis of implanted vascular cells, both of which require on the order of days to generate perfusion, they often result in compromised viability of implanted constructs. In principle, scaffolds that contain microfluidic networks (microfluidic scaffolds) can support immediate perfusion, which can then sustain the metabolism of cells that reside within the scaffold. Moreover, if the scaffold consists of a material that supports vascular cell adhesion, then it may be possible to use the microfluidic networks as templates for the growth of open, patterned vascular networks. Although many technical challenges remain, surgical anastomosis of vessels in a microfluidic scaffold to vessels in a recipient tissue bed is expected to enable immediate perfusion of the scaffold with blood upon implantation.

### Microfluidic Scaffolds for Tissue Engineering

Scaffolds for tissue engineering must be sufficiently porous to enable delivery of oxygen and nutrients to embedded cells (110). Because PDMS is impermeable to culture media [although it is permeable to water vapor and oxygen (111)], it is not a promising material for this application. Also, scaffolds should promote cell attachment (PDMS does not, unless functionalized) and should roughly match the mechanical properties of the tissue of interest (PDMS is much stiffer than most tissues).

Hydrogels represent an attractive class of scaffolds owing to their biocompatibility and tunable porosity and elastic moduli (112). Transport in microfluidic hydrogels can mimic the transport pathways in vivo, where convection through a branching network and diffusion into the surrounding tissue are dominant. Because hydrogels are porous, interstitial flow alone can be used to deliver solutes throughout a scaffold (110). This approach, however, requires a substantial hydraulic pressure that scales linearly with the length of the tissue construct; more importantly, excessive interstitial flow can decrease cell viability, possibly by exposing cells to high shear stress (113, 114).

Compared with the formation of microfluidic networks in PDMS, the formation of a single open channel (let alone an entire network) in a hydrogel requires care. In contrast to PDMS, hydrogels are separated by a film of water when placed in contact; microfluidic channels constructed by layering a patterned gel on top of a flat gel, therefore, are not leakproof (115). Under internal pressure, adherent hydrogels tend to detach from each other. Thus, much of the challenge in forming microfluidic hydrogels lies in the development of methods to ensure that the scaffolds are sufficiently strong to withstand the stresses imparted by perfusion. In seminal work by Stroock and colleagues (116), slabs of micromolded calcium alginate hydrogels were bonded onto flat layers to form a sealed structure (**Figure 5a**). Because this hydrogel requires calcium ions for electrostatic crosslinking, adding sodium citrate partially dissolved the gel by chelating

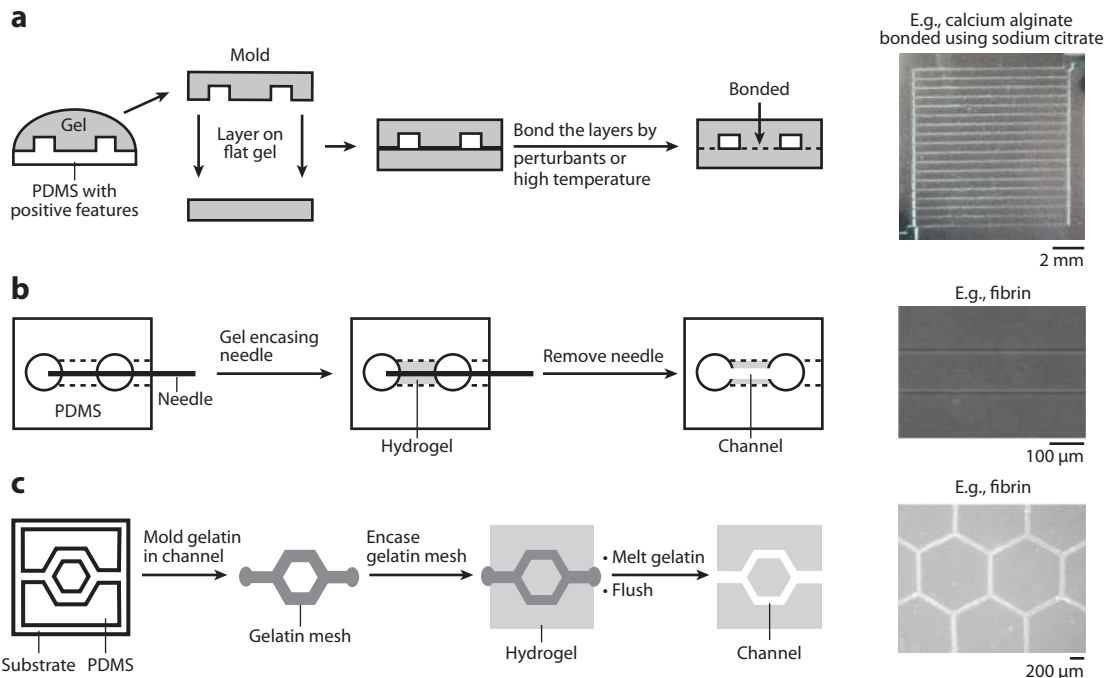


**Figure 5**

Fabrication of microfluidic hydrogels. (a) Gel bonding. Perturbants (e.g., sodium citrate for alginate gels) and high temperature bond gels by transient, partial depolymerization and transient melting, respectively. Modified with permission from the American Chemical Society (115, 116). (b) Needles may be used to form single microfluidic channels in hydrogels. Modified with permission from Elsevier (119). (c) Molded gelatin may also be used to form microfluidic networks in gels. Modified with permission from the Royal Society of Chemistry (122). Abbreviation: PDMS, polydimethylsiloxane.

calcium and allowed soluble alginate to interpenetrate the gel boundaries and eventually crosslink the two surfaces upon readdition of calcium (116). In a similar approach, transient exposure of adherent ECM-based gels (collagen and fibrin) to chaotropes such as guanidine hydrochloride resulted in gel bonding; here, the chaotropes acted as perturbants that partially depolymerized the gels (115). Other studies have relied on thermal approaches to bonding: Patterned silk fibroin gels were bonded by applying mechanical pressure to stacked layers under high temperature (70°C) with the addition of aqueous silk fibroin solution at the interface (117); transient (in seconds) melting of agarose gels also resulted in bonding (118).

An alternate strategy to bonding is to excavate the desired channels. A simple method is to mold hydrogel around removable tubular structures, such as needles (119, 120) (Figure 5b) and steel wires (121). This method, however, is limited to single channels. A more versatile technique is to use micromolded gelatin templates to form entire microfluidic networks. In this procedure, molding of concentrated (10%) gelatin solution between a patterned PDMS stamp and a flat substrate formed a gelatin mesh that could be released into solution as a free-standing structure. Gelation of collagen or fibrin around this mesh, followed by a saline flush at 37°C that removed the melted gelatin, resulted in open microfluidic networks throughout the hydrogel (Figure 5c) (122). This gelatin-based method could be used to build multiplanar networks by stacking, but the construction of truly interconnected 3D networks is technically challenging. An alternate approach is to use optical lithography to carve 3D interconnected channels inside photodegradable

**Péclet number:** a dimensionless ratio of convective to diffusive solute flux (e.g., within a vessel)

**Biot number:** a dimensionless ratio of the solute transfer resistances within a material and on its surface (e.g., within a tissue and at the tissue-vessel interface)

polyethylene glycol gels (123). This method can theoretically be extended to any polymer gel with photodegradable crosslinkers.

The enhanced transport properties of microfluidic gels make such gels particularly relevant for tissue engineering. In the absence of channels (e.g., in homogeneous scaffolds), a pressure gradient on the order of  $1 \text{ cm H}_2\text{O mm}^{-1}$  resulted in very slow interstitial flow for the transport of low-molecular-weight solutes such as rhodamine ( $MW = 479 \text{ Da}$ ) (122). With the aid of microfluidic channels, however, convective transport saturates channels and allows immediate diffusion into the gel. Similarly, these channels can accelerate solute extraction from the gel by acting as sinks (116, 122). The maintenance of a concentration profile that does not vary along the length of microchannels can be achieved with high Péclet and Biot numbers, such that the mass-transfer process is controlled solely by diffusion-reaction kinetics within the bulk of the scaffold (i.e., it is not limited by convection within the channel). When a relatively uniform concentration is desired across the entire hydrogel—for example, in the supply of oxygen or glucose—one should design channels with spacing smaller than a characteristic distance,  $\lambda = 2 \cdot \sqrt{Dc/R}$ , where  $D$  is the diffusivity of the solute in the scaffold,  $c$  is the concentration of the solute in the channel, and  $R$  is the consumption rate. When designed in this way, microfluidic networks can be used to deliver low-molecular-weight solutes, such as calcein AM, to densely seeded ( $10^7 \text{ cell ml}^{-1}$ ) scaffolds (124).

### Functional Vascularization of Microfluidic Scaffolds

Although mass transport is required to maintain viability of tissues, it is not the only function of the microvascular system. For instance, in addition to maintaining water and solute balance, the endothelial barrier effectively shields parenchymal cells from interstitial fluid shear. In vitro perfusion of tissue constructs with whole blood also requires a nonthrombogenic endothelial coating (125). In the context of tissue engineering, a microvascular bed that displays normal physiology is desired to provide the surrounding tissues with the appropriate chemical and physical signals for proper parenchymal function.

This idea has called for the vascularization of microfluidic scaffolds. One promising approach is to seed normal ECs into microfluidic channels inside collagen and fibrin gels, because such ECM-based gels provide a natural substrate for cell attachment (115, 119, 122). Under constant perfusion, the ECs in microfluidic ECM gels spread and grow to confluence inside channels to form tubes and networks (**Figure 6a**) that support perfusion. Other materials such as methacrylated gelatin gels (120) also support EC growth. Co-culture with perivascular cells has been demonstrated but did not yield vessels with a mural coat (119).

Single endothelial tubes (made from gels that contain a single channel) have served as a starting point for studying the quantitative physiology of vessels in microfluidic scaffolds (119, 126). Microvessels of 50–150- $\mu\text{m}$  diameters were perfused under physiological shear stress levels of  $\sim 10 \text{ dyn cm}^{-2}$  with dextran-supplemented media that matched plasma in its viscosity ( $\sim 1.4 \text{ cP}$ ). Under basal culture conditions, these tubes displayed a barrier function that was consistent with the nonleaky phenotype of continuous endothelium in vivo (e.g., in vessels from dermis or muscle). Upon stimulation with inflammatory cytokines, the tubes reacted with loss of barrier function (**Figure 6b**) and supported leukocyte adhesion (**Figure 6c**) (119).

Single endothelial tubes have also enabled the study of how chemical and mechanical signals that are derived from perfusion alter the phenotype of vessels (127, 128). Higher levels of the second messenger cyclic AMP (a result of supplementing the perfusate with a membrane-permeable analog) caused lower permeabilities to albumin and higher charge selectivities; the latter may indicate the presence of a functional glycocalyx on the vascular lumen. Likewise, exposure of



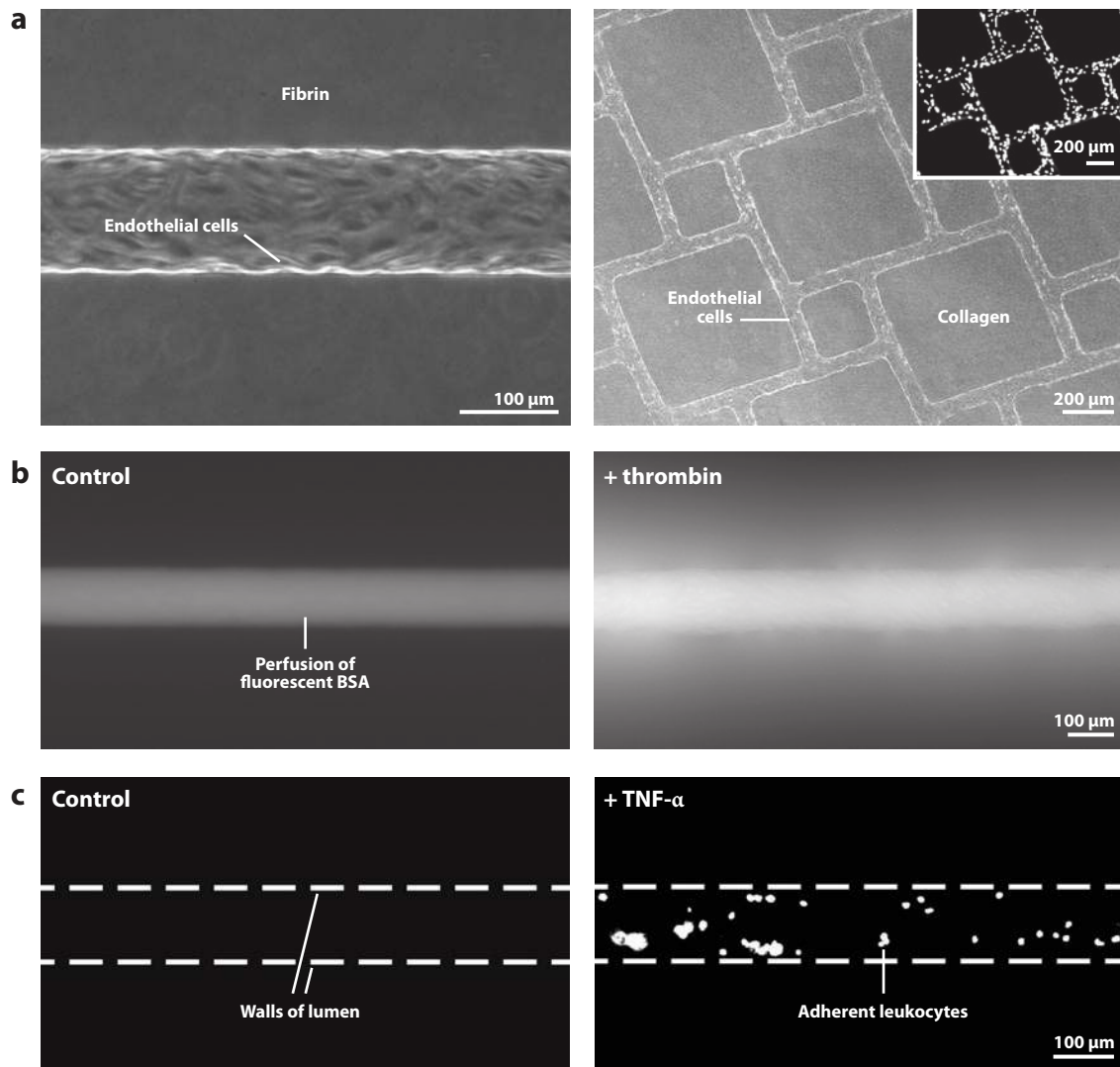


**Figure 6**

Vascularization of microfluidic hydrogels. (a) Extracellular matrix-based microfluidic gels provide a natural substrate for cell growth. Endothelial cells formed confluent monolayers in single channels (*left*) or networks (*right*). (*Right, inset*) Stained cell nuclei. Modified with permission from the Royal Society of Chemistry (122). (b) Perfusion of fluorescent solutes (in this case, albumin) into endothelial tubes in the study of vascular permeability. Thrombin stimulation resulted in the loss of barrier function, as demonstrated by the rapid leakage of albumin. (c) Stimulation of endothelial tubes with tumor necrosis factor  $\alpha$  (TNF- $\alpha$ ) resulted in adhesion of labeled leukocytes. (b,c) Modified with permission from Elsevier (119). Abbreviation: BSA, bovine serum albumin.

vessels to higher shear stresses led to lower permeabilities. Both high levels of cyclic AMP and high shear greatly augmented the stability of the vessel and supported long-term perfusion to at least two weeks. Vascular stability appears to require a positive transmural pressure, which serves to lower the tensile stress at the EC-scaffold interface, and a nonleaky vessel wall, which enables the transmural pressure to be sustained (127). When saturating levels of cyclic AMP were present in the perfusate, normalization of barrier function was accompanied by normalization of

EC turnover to 0.05–0.1% h<sup>-1</sup> (128), which approaches levels found in quiescent microvessels in vivo (129, 130).

The aforementioned physiological studies used primarily microfluidic collagen gels that did not contain nonvascular cells within the bulk of the scaffold. It will be important to determine to what extent these findings can be extended to other types of microfluidic scaffolds and in the presence of surrounding parenchymal cells.

A different approach to vascularization used the microfluidic networks within the hydrogel as templates for host angiogenesis upon implantation (131). In collagen scaffolds, 100- $\mu$ m pores induce significantly higher cellular invasion and vascularization than did 200- $\mu$ m and 400- $\mu$ m pores; this result may stem from the higher bending stiffness of 100- $\mu$ m pores. The higher cell density within the pores may then induce hypoxia and VEGF expression that enhances angiogenesis. By bypassing the need for in vitro vascularization, this work demonstrates an interesting approach to promote therapeutic angiogenesis within microfluidic scaffolds if perfusion is not required immediately.

## FUTURE DIRECTIONS

Although microfluidic models represent a tremendous advance in creating physiologically relevant models for the vascular system, limitations exist. For instance, as a cell-culture substrate, PDMS, which is the most common material used in constructing microfluidic devices, chemically and physically differs from the ECM. This limitation can be overcome by using various hydrogels, but even these materials fail to reproduce many of the important biochemical and biophysical characteristics of the basement membrane and interstitial matrix. Furthermore, the straight microfluidic channels with rectangular cross sections imprinted on a 2D planar surface bear little resemblance to the tortuous channels with round cross sections that characterize microvascular beds in vivo. Such differences can lead to abnormal behaviors in the microfluidic system. For instance, because leukocytes preferentially marginate toward the four corners in rectangular channels, margination of these cells at bifurcations was drastically different from that in channels with a circular cross section (132).

An important artifact of routine cell culture is the high ambient oxygen level (21%). In the microcirculation, oxygen levels rarely exceed 10% (133), and cells cultured in high oxygen levels exhibit a shorter lifespan that results from cellular senescence (134) and oxidative damage to DNA (135). Therefore, in vitro studies of vascular function or pathology, especially those phenomena that involve oxidative stress (e.g., ischemia/reperfusion injury and atherosclerosis), should strive to use oxygen levels representative of in vivo conditions. Oxygen tension can be controlled using microfluidic chips (136), but these methods have not been widely adopted. Also, measurements are needed to quantify the extent to which cellular consumption depletes oxygen levels in the confined dimensions of a microfluidic system.

Another critical factor is the availability of signals from other cell types. Numerous studies have demonstrated the importance of cell-cell interactions between ECs, SMCs, and pericytes to establish in vivo function. The absence of these paracrine or juxtacrine signals from most previous experiments undoubtedly introduced numerous artifacts and may explain the tendency for vascular permeability to be much higher in vitro than in vivo. This deficiency needs to be addressed.

As the models become more complex and sophisticated, so too will our need to actively probe cell function and signaling. Much of the information currently gleaned from microfluidic systems comes from various imaging modalities. Although these methods have provided useful insight, they are often limited in terms of their ability to provide quantitative, spatiotemporal information on cellular processes. There is now an enormous opportunity to improve existing methods

or to develop entirely new methods for monitoring the dynamics of single cells or interacting populations.

Finally, microvascular functions are in large part regulated by a variety of factors ranging from local mechanical stresses and cytokine gradients to systemically circulating hormones, and for this reason, *in vitro* techniques may never entirely suffice. It is important to recognize that, although *in vitro* microfluidic technology has provided researchers with many new tools, the combination of *in vitro* data with *in vivo* models is ultimately necessary to evaluate experimental results meaningfully.

### Filling in the Missing Pieces for a “Complete” Microvessel

With the existing techniques in hand, what are some concrete next steps for vascular models? Microfluidic models of the lymphatic system are poorly developed (126), despite the importance of lymphatics in drainage of tissues, interstitial transport, and the immune response (137, 138). The sparing flows in the lymphatic system can be difficult to generate and control, as these flow rates can be similar in magnitude to evaporation rates through PDMS; external osmotic pumps may prove useful to generate flow on the order of nanoliters per second that is relevant to lymphatics (139). Another important advance would be the formation of microfluidic models of arterioles or arteries to allow the studies of vasomotion. More realistic ECM composition, including the addition of basement membrane (Matrigel is only an approximation to actual basement membrane), elastin, and glycosaminoglycans, with *in vivo*-like material properties such as stiffness and porosity, would also be desirable. Integrating the above components would more realistically recreate the “complete” microvessel as described in standard physiology textbooks.

### Toward Functional Microvascular Beds and Tissue-Engineered Organs

A particularly attractive prospect is to grow complete and functional microvascular networks *in vitro*. As of now, perfusable *in vitro* vascular networks are limited to those preformed in microfluidic hydrogels, and these methods are yet to be widely practiced. Vascular networks formed by angiogenic sprouting, however, arise from a self-organized, physiologically relevant vascularization process that has been extensively studied *in vivo*. When forming stable, perfused microvascular networks becomes a routine procedure, one can envision co-culturing with other organ-specific cell types to produce even greater realism in organ-on-chip systems. The challenge then will be to maintain phenotypic stability of the cells so that the systems are both more physiologic and capable of being used for long-term studies.

As the major site for inflammatory responses and immune cell trafficking, the microvasculature is indispensable for modeling numerous pathological processes. Such models would benefit from vessels that exhibit organ-specific functions; an attractive target may be the formation of the discontinuous endothelium that characterizes lymphoid organs. It may be possible to promote organ-specific endothelial functions using organ-specific ECM, as has been shown with the development of fenestrated endothelium on kidney cell-derived matrix (140). More recently, the successful vascularization of decellularized hearts and lungs suggests that ECM specificity in modulating vascular function may be a general phenomenon (141, 142).

An important means of gaining insight into microvascular function is by applying multiscale computational models to simulate processes ranging from intracellular signaling, to cell-cell and cell-matrix interactions, and to communication between populations of different cell types. Such models unify our ever-increasing knowledge about vascular function and angiogenesis, and can generate testable hypotheses about the underlying biological processes. Although examples of

multiscale vascular models exist, they have only recently been applied to processes such as angiogenesis in a microfluidic system, and are still at an early stage of development (143, 144).

Ultimately, one can suggest adding components so that the complexity of the model tissues/organs approaches that of organs in vivo. A short-term objective might be to create multiple interacting organoids, thereby capturing some degree of the interplay that naturally occurs in an entire organism (145). A rational and elegant approach, we believe, is to create the simplest models that reproduce the critical functions of interest, thus avoiding the confounding variables often found in animal studies.

## DISCLOSURE STATEMENT

The authors are not aware of any affiliations, memberships, funding, or financial holdings that might be perceived as affecting the objectivity of this review.

## ACKNOWLEDGMENTS

We thank Choong Kim for producing the 3D illustrative artwork in **Figure 1**. J.M.C. is supported by a postdoctoral fellowship from the Agency for Science, Technology and Research (A\*STAR), Singapore, and a L'Oreal-UNESCO for Women in Science Fellowship. Support to R.D.K. from the National Science Foundation (Science and Technology Center on Emergent Behaviors of Integrated Cellular Systems; CBET-0939511) and the Singapore-MIT Alliance for Research and Technology and to J.T. from the National Institute of Biomedical Imaging and Bioengineering (EB005792) and the National Heart, Lung, and Blood Institute (HL092335) is gratefully acknowledged.

## LITERATURE CITED

1. Folkman J, Haudenschild CC, Zetter BR. 1979. Long-term culture of capillary endothelial cells. *Proc. Natl. Acad. Sci. USA* 76:5217–21
2. Gitlin JD, D'Amore PA. 1983. Culture of retinal capillary cells using selective growth media. *Microvasc. Res.* 26:74–80
3. Jaffe EA, Nachman RL, Becker CG, Minick CR. 1973. Culture of human endothelial cells derived from umbilical veins. Identification by morphologic and immunologic criteria. *J. Clin. Investig.* 52:2745–56
4. Ross R. 1971. The smooth muscle cell. II. Growth of smooth muscle in culture and formation of elastic fibers. *J. Cell Biol.* 50:172–86
5. Vailhé B, Vittet D, Feige JJ. 2001. In vitro models of vasculogenesis and angiogenesis. *Lab. Investig.* 81:439–52
6. Dai G, Kaazempur-Mofrad MR, Natarajan S, Zhang Y, Vaughn S, et al. 2004. Distinct endothelial phenotypes evoked by arterial waveforms derived from atherosclerosis-susceptible and -resistant regions of human vasculature. *Proc. Natl. Acad. Sci. USA* 101:14871–76
7. Alcaide P, Auerbach S, Lusinskas FW. 2009. Neutrophil recruitment under shear flow: It's all about endothelial cell rings and gaps. *Microcirculation* 16:43–57
8. López JA, Dong JF. 2005. Shear stress and the role of high molecular weight von Willebrand factor multimers in thrombus formation. *Blood Coagul. Fibrinolysis* 16(Suppl. 1):S11–16
9. Curry FR, Adamson RH. 2010. Vascular permeability modulation at the cell, microvessel, or whole organ level: towards closing gaps in our knowledge. *Cardiovasc. Res.* 87:218–29
10. Kokura S, Yoshida N, Yoshikawa T. 2002. Anoxia/reoxygenation-induced leukocyte-endothelial cell interactions. *Free Radic. Biol. Med.* 33:427–32
11. Swartz MA, Fleury ME. 2007. Interstitial flow and its effects in soft tissues. *Annu. Rev. Biomed. Eng.* 9:229–56

12. Ruhrberg C, Gerhardt H, Golding M, Watson R, Ioannidou S, et al. 2002. Spatially restricted patterning cues provided by heparin-binding VEGF-A control blood vessel branching morphogenesis. *Genes Dev.* 16:2684–98
13. Gimbrone MA Jr, Cotran RS, Folkman J. 1974. Human vascular endothelial cells in culture. Growth and DNA synthesis. *J. Cell Biol.* 60:673–84
14. Squires TM, Quake SR. 2005. Microfluidics: fluid physics at the nanoliter scale. *Rev. Mod. Phys.* 77:977–1026
15. Stone HA, Stroock AD, Ajdari A. 2004. Engineering flows in small devices: microfluidics toward a lab-on-a-chip. *Annu. Rev. Fluid Mech.* 36:381–411
16. Kenis PJ, Ismagilov RF, Whitesides GM. 1999. Microfabrication inside capillaries using multiphase laminar flow patterning. *Science* 285:83–85
17. Takayama S, McDonald JC, Ostuni E, Liang MN, Kenis PJ, et al. 1999. Patterning cells and their environments using multiple laminar fluid flows in capillary networks. *Proc. Natl. Acad. Sci. USA* 96:5545–48
18. Vickerman V, Blundo J, Chung S, Kamm R. 2008. Design, fabrication and implementation of a novel multi-parameter control microfluidic platform for three-dimensional cell culture and real-time imaging. *Lab Chip* 8:1468–77
19. Yen RT, Fung YC. 1978. Effect of velocity of distribution on red cell distribution in capillary blood vessels. *Am. J. Physiol.* 235:H251–57
20. Schmid-Schönbein GW, Fung YC, Zweifach BW. 1975. Vascular endothelium-leukocyte interaction; sticking shear force in venules. *Circ. Res.* 36:173–84
21. Gaehtgens P, Will G, Schmidt F. 1981. Comparative rheology of nucleated and non-nucleated red blood cells. II. Rheological properties of avian red cells suspensions in narrow capillaries. *Pflügers Arch.* 390:283–87
22. Schmid-Schönbein GW, Usami S, Skalak R, Chien S. 1980. The interaction of leukocytes and erythrocytes in capillary and postcapillary vessels. *Microvasc. Res.* 19:45–70
23. Goldsmith HL, Cokelet GR, Gaehtgens P. 1989. Robin Fåhræus: evolution of his concepts in cardiovascular physiology. *Am. J. Physiol.* 257:H1005–15
24. Weinbaum S, Tarbell JM, Damiano ER. 2007. The structure and function of the endothelial glycocalyx layer. *Annu. Rev. Biomed. Eng.* 9:121–67
25. Cokelet GR, Soave R, Pugh G, Rathbun L. 1993. Fabrication of in vitro microvascular blood flow systems by photolithography. *Microvasc. Res.* 46:394–400
26. Duffy DC, McDonald JC, Schueller OJ, Whitesides GM. 1998. Rapid prototyping of microfluidic systems in poly(dimethylsiloxane). *Anal. Chem.* 70:4974–84
27. Shevkoplyas SS, Gifford SC, Yoshida T, Bitensky MW. 2003. Prototype of an in vitro model of the microcirculation. *Microvasc. Res.* 65:132–36
28. Quinn DJ, Pivkin I, Wong SY, Chiam KH, Dao M, et al. 2011. Combined simulation and experimental study of large deformation of red blood cells in microfluidic systems. *Ann. Biomed. Eng.* 39:1041–50
29. Yap B, Kamm RD. 2005. Mechanical deformation of neutrophils into narrow channels induces pseudopod projection and changes in biomechanical properties. *J. Appl. Physiol.* 98:1930–39
30. Yap B, Kamm RD. 2005. Cytoskeletal remodeling and cellular activation during deformation of neutrophils into narrow channels. *J. Appl. Physiol.* 99:2323–30
31. Shevkoplyas SS, Yoshida T, Munn LL, Bitensky MW. 2005. Biomimetic autoseparation of leukocytes from whole blood in a microfluidic device. *Anal. Chem.* 77:933–37
32. Jain A, Munn LL. 2009. Determinants of leukocyte margination in rectangular microchannels. *PLoS ONE* 4:e7104
33. Forouzan O, Burns JM, Robichaux JL, Murfee WL, Shevkoplyas SS. 2011. Passive recruitment of circulating leukocytes into capillary sprouts from existing capillaries in a microfluidic system. *Lab Chip* 11:1924–32
34. Lichtman MA. 1973. Rheology of leukocytes, leukocyte suspensions, and blood in leukemia. Possible relationship to clinical manifestations. *J. Clin. Investig.* 52:350–58
35. Bunn HF. 1997. Pathogenesis and treatment of sickle cell disease. *N. Engl. J. Med.* 337:762–69

36. Piagnerelli M, Boudjeltia KZ, Vanhaeverbeek M, Vincent JL. 2003. Red blood cell rheology in sepsis. *Intensive Care Med.* 29:1052–61
37. Mills JP, Diez-Silva M, Quinn DJ, Dao M, Lang MJ, et al. 2007. Effect of plasmodial RESA protein on deformability of human red blood cells harboring *Plasmodium falciparum*. *Proc. Natl. Acad. Sci. USA* 104:9213–17
38. Schmid-Schönbein H, Volger E. 1976. Red-cell aggregation and red-cell deformability in diabetes. *Diabetes* 25:897–902
39. Fischer TM, Haest CW, Stohr M, Kamp D, Deuticke B. 1978. Selective alteration of erythrocyte deformability by SH-reagents: evidence for an involvement of spectrin in membrane shear elasticity. *Biochim. Biophys. Acta* 510:270–82
40. Usami S, Chien S, Bertles JF. 1975. Deformability of sickle cells as studied by microsieving. *J. Lab. Clin. Med.* 86:274–79
41. Aarts PA, Heethaar RM, Sixma JJ. 1984. Red blood cell deformability influences platelets–vessel wall interaction in flowing blood. *Blood* 64:1228–33
42. Driessen GK, Scheidt-Bleichert H, Sobota A, Inhoffen W, Heidtmann H, et al. 1982. Capillary resistance to flow of hardened (diamide treated) red blood cells (RBC). *Pflügers Arch.* 392:261–67
43. Schmid-Schönbein H, Gaehtgens P. 1981. What is red cell deformability? *Scand. J. Clin. Lab. Investig. Suppl.* 156:13–26
44. Forsyth AM, Wan J, Ristenpart WD, Stone HA. 2010. The dynamic behavior of chemically “stiffened” red blood cells in microchannel flows. *Microvasc. Res.* 80:37–43
45. Shevkoplyas SS, Yoshida T, Gifford SC, Bitensky MW. 2006. Direct measurement of the impact of impaired erythrocyte deformability on microvascular network perfusion in a microfluidic device. *Lab Chip* 6:914–20
46. Higgins JM, Eddington DT, Bhatia SN, Mahadevan L. 2007. Sickle cell vasoocclusion and rescue in a microfluidic device. *Proc. Natl. Acad. Sci. USA* 104:20496–500
47. Rosenbluth MJ, Lam WA, Fletcher DA. 2008. Analyzing cell mechanics in hematologic diseases with microfluidic biophysical flow cytometry. *Lab Chip* 8:1062–70
48. Porcu P, Cripe LD, Ng EW, Bhatia S, Danielson CM, et al. 2000. Hyperleukocytic leukemias and leukostasis: a review of pathophysiology, clinical presentation and management. *Leuk. Lymphoma* 39:1–18
49. Zweifach BW, Lipowsky HH. 1984. Pressure–flow relations in blood and lymph microcirculation. In *Handbook of Physiology; Section 2: The Cardiovascular System*, ed. EM Renkin, CC Michel, pp. 251–307. Bethesda, MD: Am. Physiol. Soc.
50. Chiu JJ, Chien S. 2011. Effects of disturbed flow on vascular endothelium: pathophysiological basis and clinical perspectives. *Physiol. Rev.* 91:327–87
51. Davies PF. 1995. Flow-mediated endothelial mechanotransduction. *Physiol. Rev.* 75:519–60
52. Chau L, Doran M, Cooper-White J. 2009. A novel multishear microdevice for studying cell mechanics. *Lab Chip* 9:1897–902
53. Tsou JK, Gower RM, Ting HJ, Schaff UY, Insana MF, et al. 2008. Spatial regulation of inflammation by human aortic endothelial cells in a linear gradient of shear stress. *Microcirculation* 15:311–23
54. Gu W, Zhu X, Futai N, Cho BS, Takayama S. 2004. Computerized microfluidic cell culture using elastomeric channels and Braille displays. *Proc. Natl. Acad. Sci. USA* 101:15861–66
55. Song JW, Gu W, Futai N, Warner KA, Nor JE, Takayama S. 2005. Computer-controlled microcirculatory support system for endothelial cell culture and shearing. *Anal. Chem.* 77:3993–99
56. Michel CC, Curry FE. 1999. Microvascular permeability. *Physiol. Rev.* 79:703–61
57. Albelda SM, Sampson PM, Haselton FR, McNiff JM, Mueller SN, et al. 1988. Permeability characteristics of cultured endothelial cell monolayers. *J. Appl. Physiol.* 64:308–22
58. Jo H, Dull RO, Hollis TM, Tarbell JM. 1991. Endothelial albumin permeability is shear dependent, time dependent, and reversible. *Am. J. Physiol.* 260:H1992–96
59. Young EW, Watson MW, Srigunapalan S, Wheeler AR, Simmons CA. 2010. Technique for real-time measurements of endothelial permeability in a microfluidic membrane chip using laser-induced fluorescence detection. *Anal. Chem.* 82:808–16

60. Shao J, Wu L, Wu J, Zheng Y, Zhao H, et al. 2009. Integrated microfluidic chip for endothelial cells culture and analysis exposed to a pulsatile and oscillatory shear stress. *Lab Chip* 9:3118–25
61. Shao J, Wu L, Wu J, Zheng Y, Zhao H, et al. 2010. A microfluidic chip for permeability assays of endothelial monolayer. *Biomed. Microdevices* 12:81–88
62. Douville NJ, Tung YC, Li R, Wang JD, El-Sayed ME, Takayama S. 2010. Fabrication of two-layered channel system with embedded electrodes to measure resistance across epithelial and endothelial barriers. *Anal. Chem.* 82:2505–11
63. Gordon JL. 1986. Extracellular ATP: effects, sources and fate. *Biochem. J.* 233:309–19
64. Sprague RS, Ellsworth ML, Stephenson AH, Lonigro AJ. 1996. ATP: the red blood cell link to NO and local control of the pulmonary circulation. *Am. J. Physiol.* 271:H2717–22
65. Edwards J, Sprung R, Sprague R, Spence D. 2001. Chemiluminescence detection of ATP release from red blood cells upon passage through microbore tubing. *Analyst* 126:1257–60
66. Price AK, Fischer DJ, Martin RS, Spence DM. 2004. Deformation-induced release of ATP from erythrocytes in a poly(dimethylsiloxane)-based microchip with channels that mimic resistance vessels. *Anal. Chem.* 76:4849–55
67. Price AK, Martin RS, Spence DM. 2006. Monitoring erythrocytes in a microchip channel that narrows uniformly: towards an improved microfluidic-based mimic of the microcirculation. *J. Chromatogr. A* 1111:220–27
68. Moehlenbrock MJ, Price AK, Martin RS. 2006. Use of microchip-based hydrodynamic focusing to measure the deformation-induced release of ATP from erythrocytes. *Analyst* 131:930–37
69. Forsyth AM, Wan J, Owrutsky PD, Abkarian M, Stone HA. 2011. Multiscale approach to link red blood cell dynamics, shear viscosity, and ATP release. *Proc. Natl. Acad. Sci. USA* 108:10986–91
70. Wan J, Ristenpart WD, Stone HA. 2008. Dynamics of shear-induced ATP release from red blood cells. *Proc. Natl. Acad. Sci. USA* 105:16432–37
71. Chien S. 1987. Red cell deformability and its relevance to blood flow. *Annu. Rev. Physiol.* 49:177–92
72. Ignarro LJ, Buga GM, Wood KS, Byrns RE, Chaudhuri G. 1987. Endothelium-derived relaxing factor produced and released from artery and vein is nitric oxide. *Proc. Natl. Acad. Sci. USA* 84:9265–69
73. Taha Z, Kiechle F, Malinski T. 1992. Oxidation of nitric oxide by oxygen in biological systems monitored by porphyrinic sensor. *Biochem. Biophys. Res. Commun.* 188:734–39
74. Kotsis DH, Spence DM. 2003. Detection of ATP-induced nitric oxide in a biomimetic circulatory vessel containing an immobilized endothelium. *Anal. Chem.* 75:145–51
75. Spence DM, Torrence NJ, Kovarik ML, Martin RS. 2004. Amperometric determination of nitric oxide derived from pulmonary artery endothelial cells immobilized in a microchip channel. *Analyst* 129:995–1000
76. D'Amico Oblak T, Root P, Spence DM. 2006. Fluorescence monitoring of ATP-stimulated, endothelium-derived nitric oxide production in channels of a poly(dimethylsiloxane)-based microfluidic device. *Anal. Chem.* 78:3193–97
77. Genes LI, Tolan NV, Hulvey MK, Martin RS, Spence DM. 2007. Addressing a vascular endothelium array with blood components using underlying microfluidic channels. *Lab Chip* 7:1256–59
78. Letourneau S, Hernandez L, Faris AN, Spence DM. 2010. Evaluating the effects of estradiol on endothelial nitric oxide stimulated by erythrocyte-derived ATP using a microfluidic approach. *Anal. Bioanal. Chem.* 397:3369–75
79. Vogel PA, Halpin ST, Martin RS, Spence DM. 2011. Microfluidic transendothelial electrical resistance measurement device that enables blood flow and postgrowth experiments. *Anal. Chem.* 83:4296–301
80. Nemerson Y, Turitto VT. 1991. The effect of flow on hemostasis and thrombosis. *Thromb. Haemost.* 66:272–76
81. Runyon MK, Johnson-Kerner BL, Kastrop CJ, Van Ha TG, Ismagilov RF. 2007. Propagation of blood clotting in the complex biochemical network of hemostasis is described by a simple mechanism. *J. Am. Chem. Soc.* 129:7014–15
82. Kastrop CJ, Runyon MK, Shen F, Ismagilov RF. 2006. Modular chemical mechanism predicts spatiotemporal dynamics of initiation in the complex network of hemostasis. *Proc. Natl. Acad. Sci. USA* 103:15747–52

83. Shen F, Kastrup CJ, Liu Y, Ismagilov RF. 2008. Threshold response of initiation of blood coagulation by tissue factor in patterned microfluidic capillaries is controlled by shear rate. *Arterioscler. Thromb. Vasc. Biol.* 28:2035–41
84. Carmeliet P, Jain RK. 2011. Molecular mechanisms and clinical applications of angiogenesis. *Nature* 473:298–307
85. Ramsauer M, D'Amore PA. 2007. Contextual role for angiopoietins and TGF $\beta$ 1 in blood vessel stabilization. *J. Cell Sci.* 120:1810–17
86. Stalmans I, Ng YS, Rohan R, Fruttiger M, Bouche A, et al. 2002. Arteriolar and venular patterning in retinas of mice selectively expressing VEGF isoforms. *J. Clin. Investig.* 109:327–36
87. Argraves KM, Wilkerson BA, Argraves WS. 2010. Sphingosine-1-phosphate signaling in vasculogenesis and angiogenesis. *World J. Biol. Chem.* 1:291–97
88. Visentin B, Vekich JA, Sibbald BJ, Cavalli AL, Moreno KM, et al. 2006. Validation of an anti-sphingosine-1-phosphate antibody as a potential therapeutic in reducing growth, invasion, and angiogenesis in multiple tumor lineages. *Cancer Cell* 9:225–38
89. Suri C, McClain J, Thurston G, McDonald DM, Zhou H, et al. 1998. Increased vascularization in mice overexpressing angiopoietin-1. *Science* 282:468–71
90. Hangai M, Murata T, Miyawaki N, Spee C, Lim JI, et al. 2001. Angiopoietin-1 upregulation by vascular endothelial growth factor in human retinal pigment epithelial cells. *Investig. Ophthalmol. Vis. Sci.* 42:1617–25
91. Folkman J, Haudenschild C. 1980. Angiogenesis in vitro. *Nature* 288:551–56
92. Li YH, Zhu C. 1999. A modified Boyden chamber assay for tumor cell transendothelial migration in vitro. *Clin. Exp. Metastasis* 17:423–29
93. Bouhadir KH, Mooney DJ. 2001. Promoting angiogenesis in engineered tissues. *J. Drug Target.* 9:397–406
94. Davis GE, Koh W, Stratman AN. 2007. Mechanisms controlling human endothelial lumen formation and tube assembly in three-dimensional extracellular matrices. *Birth Defects Res. C Embryo Today* 81:270–85
95. Chung S, Sudo R, Vickerman V, Zervantonakis IK, Kamm RD. 2010. Microfluidic platforms for studies of angiogenesis, cell migration, and cell-cell interactions. Sixth International Bio-Fluid Mechanics Symposium and Workshop March 28–30, 2008, Pasadena, California. *Ann. Biomed. Eng.* 38:1164–77
96. Dertinger SKW, Chiu DT, Jeon NL, Whitesides GM. 2001. Generation of gradients having complex shapes using microfluidic networks. *Anal. Chem.* 73:1240–46
97. Chung S, Sudo R, Mack PJ, Wan CR, Vickerman V, Kamm RD. 2009. Cell migration into scaffolds under co-culture conditions in a microfluidic platform. *Lab Chip* 9:269–75
98. Chung S, Sudo R, Zervantonakis IK, Rimchala T, Kamm RD. 2009. Surface-treatment-induced three-dimensional capillary morphogenesis in a microfluidic platform. *Adv. Mater.* 21:4863–67
99. Barkefors I, Thorslund S, Nikolajeff F, Kreuger J. 2009. A fluidic device to study directional angiogenesis in complex tissue and organ culture models. *Lab Chip* 9:529–35
100. Gerhardt H, Golding M, Fruttiger M, Ruhrberg C, Lundkvist A, et al. 2003. VEGF guides angiogenic sprouting utilizing endothelial tip cell filopodia. *J. Cell Biol.* 161:1163–77
101. Burdick JA, Khademhosseini A, Langer R. 2004. Fabrication of gradient hydrogels using a microfluidics/photopolymerization process. *Langmuir* 20:5153–56
102. Kang H, Bayless KJ, Kaunas R. 2008. Fluid shear stress modulates endothelial cell invasion into three-dimensional collagen matrices. *Am. J. Physiol. Heart Circ. Physiol.* 295:H2087–97
103. Song JW, Munn LL. 2011. Fluid forces control endothelial sprouting. *Proc. Natl. Acad. Sci. USA* 108:15342–47
104. Korff T, Kimmina S, Martiny-Baron G, Augustin HG. 2001. Blood vessel maturation in a 3-dimensional spheroidal coculture model: direct contact with smooth muscle cells regulates endothelial cell quiescence and abrogates VEGF responsiveness. *FASEB J.* 15:447–57
105. Sudo R, Chung S, Zervantonakis IK, Vickerman V, Toshimitsu Y, et al. 2009. Transport-mediated angiogenesis in 3D epithelial coculture. *FASEB J.* 23:2155–64
106. Carrion B, Huang CP, Ghajar CM, Kachgal S, Kniazeva E, et al. 2010. Recreating the perivascular niche ex vivo using a microfluidic approach. *Biotechnol. Bioeng.* 107:1020–28



107. Hwa AJ, Fry RC, Sivaraman A, So PT, Samson LD, et al. 2007. Rat liver sinusoidal endothelial cells survive without exogenous VEGF in 3D perfused co-cultures with hepatocytes. *FASEB J.* 21:2564–79
108. Huh D, Matthews BD, Mammoto A, Montoya-Zavala M, Hsin HY, Ingber DE. 2010. Reconstituting organ-level lung functions on a chip. *Science* 328:1662–68
109. Song JW, Cavnar SP, Walker AC, Luker KE, Gupta M, et al. 2009. Microfluidic endothelium for studying the intravascular adhesion of metastatic breast cancer cells. *PLoS ONE* 4:e5756
110. Radisic M, Yang L, Boublik J, Cohen RJ, Langer R, et al. 2004. Medium perfusion enables engineering of compact and contractile cardiac tissue. *Am. J. Physiol. Heart Circ. Physiol.* 286:H507–16
111. Randall GC, Doyle PS. 2005. Permeation-driven flow in poly(dimethylsiloxane) microfluidic devices. *Proc. Natl. Acad. Sci. USA* 102:10813–18
112. Lee KY, Mooney DJ. 2001. Hydrogels for tissue engineering. *Chem. Rev.* 101:1869–79
113. Shi ZD, Ji XY, Qazi H, Tarbell JM. 2009. Interstitial flow promotes vascular fibroblast, myofibroblast, and smooth muscle cell motility in 3-D collagen I via upregulation of MMP-1. *Am. J. Physiol. Heart Circ. Physiol.* 297:H1225–34
114. Dvir T, Levy O, Shachar M, Granot Y, Cohen S. 2007. Activation of the ERK1/2 cascade via pulsatile interstitial fluid flow promotes cardiac tissue assembly. *Tissue Eng.* 13:2185–93
115. Price GM, Chu KK, Truslow JG, Tang-Schomer MD, Golden AP, et al. 2008. Bonding of macromolecular hydrogels using perturbants. *J. Am. Chem. Soc.* 130:6664–65
116. Cabodi M, Choi NW, Gleghorn JP, Lee CS, Bonassar LJ, Stroock AD. 2005. A microfluidic biomaterial. *J. Am. Chem. Soc.* 127:13788–89
117. Bettinger CJ, Cyr KM, Matsumoto A, Langer R, Borenstein JT, Kaplan DL. 2007. Silk fibroin microfluidic devices. *Adv. Mater.* 19:2847–50
118. Ling Y, Rubin J, Deng Y, Huang C, Demirci U, et al. 2007. A cell-laden microfluidic hydrogel. *Lab Chip* 7:756–62
119. Chrobak KM, Potter DR, Tien J. 2006. Formation of perfused, functional microvascular tubes in vitro. *Microvasc. Res.* 71:185–96
120. Nichol JW, Koshy ST, Bae H, Hwang CM, Yamanlar S, Khademhosseini A. 2010. Cell-laden micro-engineered gelatin methacrylate hydrogels. *Biomaterials* 31:5536–44
121. Vernon RB, Gooden MD, Lara SL, Wight TN. 2005. Native fibrillar collagen membranes of micron-scale and submicron thicknesses for cell support and perfusion. *Biomaterials* 26:1109–17
122. Golden AP, Tien J. 2007. Fabrication of microfluidic hydrogels using molded gelatin as a sacrificial element. *Lab Chip* 7:720–25
123. Kloxin AM, Kasko AM, Salinas CN, Anseth KS. 2009. Photodegradable hydrogels for dynamic tuning of physical and chemical properties. *Science* 324:59–63
124. Choi NW, Cabodi M, Held B, Gleghorn JP, Bonassar LJ, Stroock AD. 2007. Microfluidic scaffolds for tissue engineering. *Nat. Mater.* 6:908–15
125. McGuigan AP, Sefton MV. 2006. Vascularized organoid engineered by modular assembly enables blood perfusion. *Proc. Natl. Acad. Sci. USA* 103:11461–66
126. Price GM, Chrobak KM, Tien J. 2008. Effect of cyclic AMP on barrier function of human lymphatic microvascular tubes. *Microvasc. Res.* 76:46–51
127. Price GM, Wong KH, Truslow JG, Leung AD, Acharya C, Tien J. 2010. Effect of mechanical factors on the function of engineered human blood microvessels in microfluidic collagen gels. *Biomaterials* 31:6182–89
128. Wong KH, Truslow JG, Tien J. 2010. The role of cyclic AMP in normalizing the function of engineered human blood microvessels in microfluidic collagen gels. *Biomaterials* 31:4706–14
129. Engerman RL, Pfaffenbach D, Davis MD. 1967. Cell turnover of capillaries. *Lab. Invest.* 17:738–43
130. Hobson B, Denekamp J. 1984. Endothelial proliferation in tumours and normal tissues: continuous labelling studies. *Br. J. Cancer* 49:405–13
131. Zheng Y, Henderson PW, Choi NW, Bonassar LJ, Spector JA, Stroock AD. 2011. Microstructured templates for directed growth and vascularization of soft tissue in vivo. *Biomaterials* 32:5391–401
132. Yang X, Forouzan O, Burns JM, Shevkopyas SS. 2011. Traffic of leukocytes in microfluidic channels with rectangular and rounded cross-sections. *Lab Chip* 11:3231–40

133. Tsai AG, Johnson PC, Intaglietta M. 2003. Oxygen gradients in the microcirculation. *Physiol. Rev.* 83:933–63
134. Packer L, Fuehr K. 1977. Low oxygen concentration extends the lifespan of cultured human diploid cells. *Nature* 267:423–25
135. Chen Q, Fischer A, Reagan JD, Yan LJ, Ames BN. 1995. Oxidative DNA damage and senescence of human diploid fibroblast cells. *Proc. Natl. Acad. Sci. USA* 92:4337–41
136. Lam RH, Kim MC, Thorsen T. 2009. Culturing aerobic and anaerobic bacteria and mammalian cells with a microfluidic differential oxygenator. *Anal. Chem.* 81:5918–24
137. Rockson SG. 2001. Lymphedema. *Am. J. Med.* 110:288–95
138. Ryan TJ. 1989. Structure and function of lymphatics. *J. Invest. Dermatol.* 93:18S–24S
139. Park JY, Hwang CM, Lee SH. 2007. Gradient generation by an osmotic pump and the behavior of human mesenchymal stem cells under the fetal bovine serum concentration gradient. *Lab Chip* 7:1673–80
140. Milici AJ, Furie MB, Carley WW. 1985. The formation of fenestrations and channels by capillary endothelium in vitro. *Proc. Natl. Acad. Sci. USA* 82:6181–85
141. Ott HC, Matthiesen TS, Goh SK, Black LD, Kren SM, et al. 2008. Perfusion-decellularized matrix: using nature's platform to engineer a bioartificial heart. *Nat. Med.* 14:213–21
142. Petersen TH, Calle EA, Zhao L, Lee EJ, Gui L, et al. 2010. Tissue-engineered lungs for in vivo implantation. *Science* 329:538–41
143. Liu G, Qutub AA, Vempati P, Mac Gabhann F, Popel AS. 2011. Module-based multiscale simulation of angiogenesis in skeletal muscle. *Theor. Biol. Med. Model.* 8:6
144. Seaman ME, Peirce SM, Kelly K. 2011. Rapid analysis of vessel elements (RAVE): a tool for studying physiologic, pathologic and tumor angiogenesis. *PLoS ONE* 6:e20807
145. Esch MB, King TL, Shuler ML. 2011. The role of body-on-a-chip devices in drug and toxicity studies. *Annu. Rev. Biomed. Eng.* 13:55–72